

The Influence of Amazon Rainfall on the Atlantic ITCZ through Convectively Coupled Kelvin Waves

HUI WANG AND RONG FU

School of Earth and Atmospheric Sciences, Georgia Institute of Technology, Atlanta, Georgia

(Manuscript received 2 September 2005, in final form 12 June 2006)

ABSTRACT

Using outgoing longwave radiation (OLR) and Tropical Rainfall Measuring Mission (TRMM) daily rain-rate data, systematic changes in intensity and location of the Atlantic intertropical convergence zone (ITCZ) were detected along the equator during boreal spring. It is found that the changes in convection over the tropical Atlantic may be induced by deep convection in equatorial South America. Lagged regression analyses demonstrate that the anomalies of convection developed over the land propagate eastward across the Atlantic and then into Africa. The eastward-propagating disturbances appear to be convectively coupled Kelvin waves with a period of 6–7.5 days and a phase speed of around 15 m s^{-1} . These waves modulate the intensity and location of the convection in the tropical Atlantic and result in a zonal variation of the Atlantic ITCZ on synoptic time scales. The convectively coupled Kelvin wave has substantial signals in both the lower and upper troposphere. Both a reanalysis dataset and the Quick Scatterometer (QuikSCAT) ocean surface wind are used to characterize the Kelvin wave. This study suggests that synoptic-scale variation of the Atlantic ITCZ may be linked to precipitation anomalies in South America through the convectively coupled Kelvin wave. The results imply that the changes of Amazon convection could contribute to the large variability of the tropical Atlantic ITCZ observed during boreal spring.

1. Introduction

The Atlantic intertropical convergence zone (ITCZ) exhibits large variations on seasonal to interannual and decadal time scales. These variations influence the climate of adjacent continents especially over northeast Brazil and West Africa (Hastenrath and Heller 1977; Lamb 1978; Enfield 1996; Janicot et al. 1998; Robertson et al. 2004; Uvo et al. 1998) and interact with the North Atlantic Oscillation (NAO; Robertson et al. 2000; Okumura et al. 2001; Czaja et al. 2002; Liu et al. 2004). Its seasonal variation is characterized by a significant meridional migration of convection and precipitation, as shown in Fig. 1, which is represented by long-term seasonal mean outgoing longwave radiation (OLR) from an interpolated OLR dataset provided by the Climate Diagnostics Center (CDC; Liebmann and Smith 1996). Although insolation and the Atlantic sea surface temperature (SST) fundamentally drive the sea-

sonal changes of the Atlantic ITCZ (e.g., Mitchell and Wallace 1992; Li and Philander 1997; Fu et al. 2001; Biasutti et al. 2003; Okumura and Xie 2004), external influences from, for example, El Niño–Southern Oscillation (ENSO) and NAO significantly contribute to the climate variability of the Atlantic ITCZ. For example, the eastern Pacific SST anomalies associated with the ENSO lead to changes in surface wind over the tropical Atlantic (e.g., Hastenrath and Heller 1977; Moura and Shukla 1981; Enfield 1996; Saravanan and Chang 2000; Chiang et al. 2002). The latter can be amplified by local air–sea interaction and becomes a main cause of the interannual changes of SST and the ITCZ in the tropical Atlantic (e.g., Chang et al. 1997, 2000; Huang et al. 2002). The decadal variability of the Atlantic ITCZ arises from a strong tropical–extratropical interaction in the Atlantic (Rajagopalan et al. 1998; Xie and Tanimoto 1998; Xie 1999; Dima et al. 2001) and an external influence of the decadal variability in the tropical Pacific (Chiang et al. 2000; Cobb et al. 2001).

The Atlantic Ocean is flanked by two large tropical continents where major atmospheric convection centers are located. An empirical analysis of historical observational records also suggests that the interannual

Corresponding author address: Dr. Hui Wang, School of Earth and Atmospheric Sciences, Georgia Institute of Technology, 311 Ferst Drive, Atlanta, GA 30332-0340.
E-mail: huiwang@eas.gatech.edu

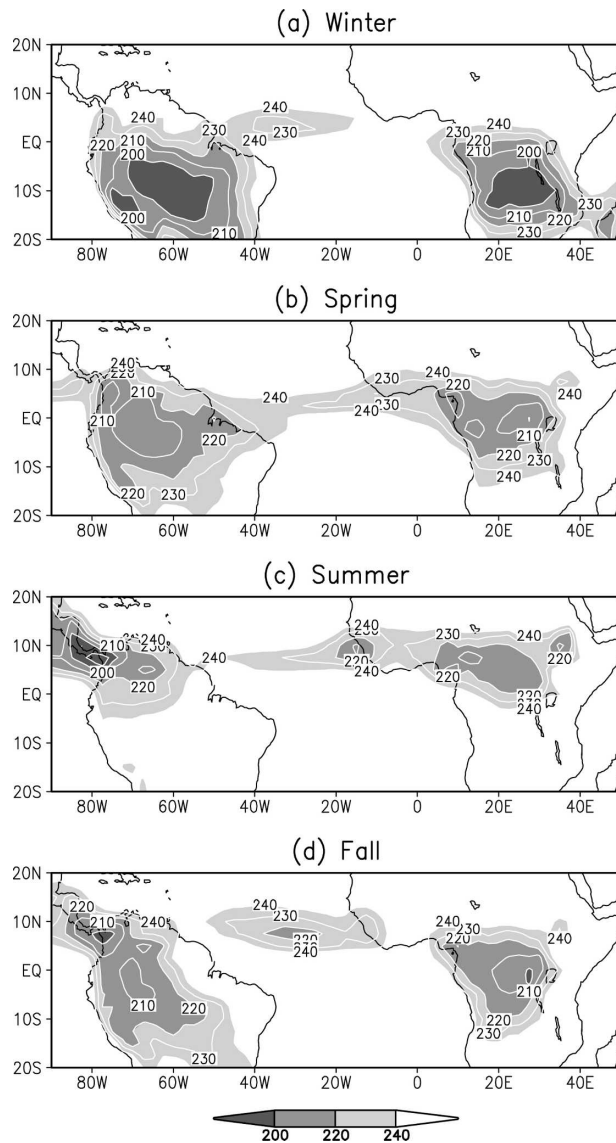


FIG. 1. Climatological seasonal mean OLR averaged over the period 1979–93 for (a) boreal winter, (b) spring, (c) summer, and (d) fall, showing low OLR ($<240 \text{ W m}^{-2}$) only. Contour interval is 10 W m^{-2} . Light, dark, and darker shadings indicate OLR below 240, 220, and 200 W m^{-2} , respectively.

variation of South American rainfall could have a significant influence on SST anomalies in part of the tropical Atlantic (Poveda and Mesa 1997). The potential importance of the adjacent landmasses in determining climate variability over the tropical Atlantic has been increasingly recognized in recent years (e.g., Xie and Carton 2004; Hagos and Cook 2005). However, because of the lack of clear observational evidence and discrepancies among different numerical model results a clear consensus has not been reached as to whether and how convection over tropical South America would have a

significant influence on the SST and ITCZ over the tropical Atlantic. For example, numerical simulations of Biasutti et al. (2003, 2005) suggest that the seasonal changes in precipitation over South America and Africa may alter the instability of the atmosphere over the tropical Atlantic and influence the annual march of the Atlantic ITCZ. However, by analyzing different numerical model experiments, Ruiz-Barradas et al. (2003) have suggested that the continental heating from the Amazon appears to be unimportant. To clarify the role of South American convection, we examine the link between convection over South America and the Atlantic ITCZ and explore the underlying atmospheric dynamic processes using satellite observations and reanalysis of atmospheric circulation product.

Any influence of convective heating over South America on the Atlantic ITCZ should be carried out by atmospheric waves on synoptic to intraseasonal time scales. Such an influence thus would be detected more clearly on these time scales when other slower influences especially from underlying SST anomalies would be minimal. A substantial portion of convection in the Atlantic ITCZ is modulated by synoptic-scale disturbances (Gu and Zhang 2001, 2002). These disturbances are generally zonal propagating waves, which may cause significant zonal variation of convection and precipitation in the ITCZ. Figure 2 presents an example of eastward-propagating convective disturbance in the Atlantic ITCZ from 16 April to 22 April 1993 using the CDC's interpolated daily OLR data (Liebmann and Smith 1996). On 16 April, the deepest convection is located in South America along the equator. By 17 April, the convective envelope has shifted eastward to the western Atlantic. The convective disturbances continue to shift eastward over the next 4 days and reach Africa on 22 April. During this 7-day period the Atlantic ITCZ undergoes significant changes in the zonal position of deep convection. The observational evidence raises questions as to what causes the zonal variation of the Atlantic ITCZ and how the zonal variation of the ITCZ relates to precipitation in South America and Africa.

Using long-term twice-daily OLR data, Wheeler and Kiladis (1999) and Wheeler et al. (2000) document various tropical wave modes that are strongly coupled with deep convection. They find that the convectively coupled Kelvin wave represents the most significant part of the total OLR variance, which is more than any other tropical waves over equatorial South America, the Atlantic, and Africa. Early evidence of Kelvin waves crossing equatorial South America and the Atlantic as convectively coupled disturbances was documented by Dunkerton and Crum (1995), though their

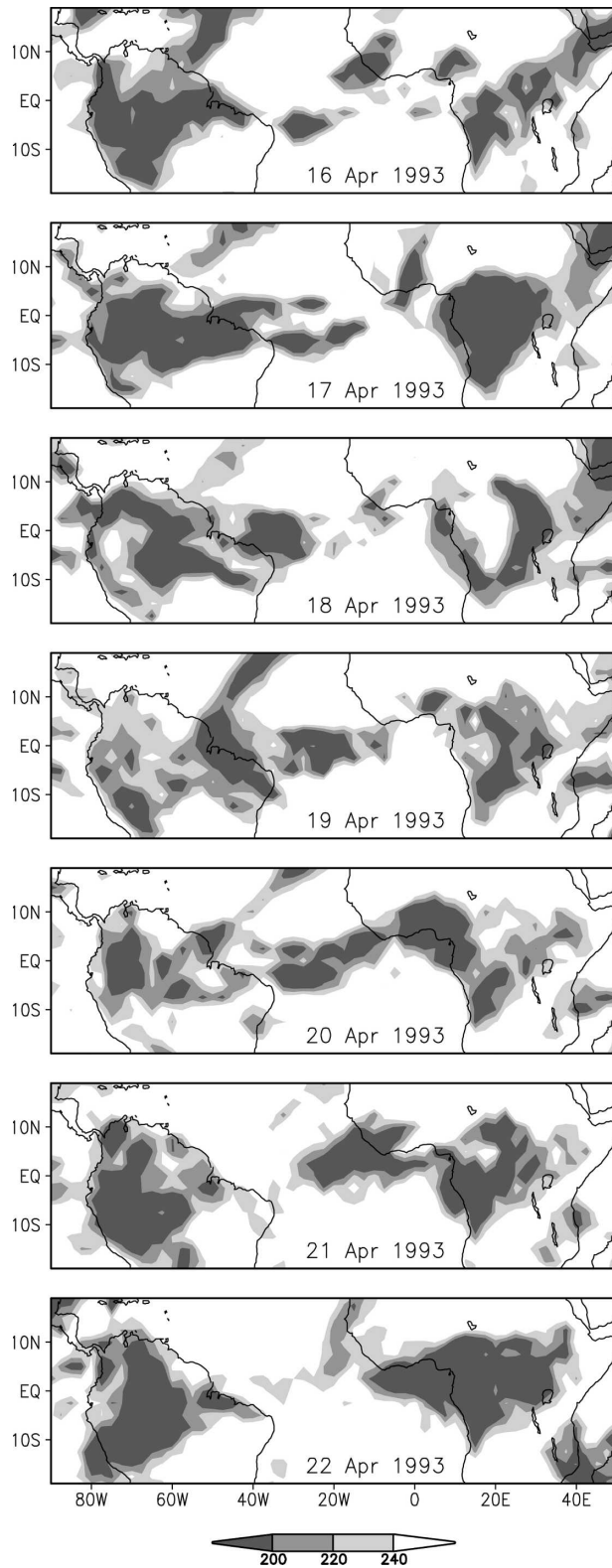


FIG. 2. Daily OLR for 16–22 Apr 1993. Light, dark, and darker shadings indicate OLR below 240, 220, and 200 W m^{-2} , respectively.

emphasis was placed on the 2–15-day equatorial convection in the Indian Ocean and the western Pacific. The longitude–time diagram of 10-yr (1980–89) daily OLR near the equator shown in Dunkerton and Crum (1995, their Fig. 1) reveals a distinct seasonality of the eastward-propagating convection over the South American and Atlantic sectors. Serra and Houze (2002) and Straub and Kiladis (2002) also present case studies of a convectively coupled Kelvin wave in the eastern Pacific ITCZ. They demonstrate that the eastward-propagating Kelvin wave exerts a strong control on local convection and precipitation along the eastern Pacific ITCZ. The equatorially trapped waves appear most frequently (Dunkerton and Crum 1995) and also exhibit maximum variability (Roundy and Frank 2004) in boreal spring. In addition, both Amazon convection and the Atlantic ITCZ are closest to the equator (Fig. 1b) in this season. Therefore, we will focus on boreal spring, March–May (MAM), to explore whether the convectively coupled Kelvin wave can modulate synoptic variations of convection and precipitation in the tropical Atlantic and cause the zonal variation of the Atlantic ITCZ as shown in Fig. 2. In particular, we will clarify whether the Kelvin waves in this case originate from deep convection in equatorial South America, then propagate eastward across the Atlantic and Africa, and thus link convection and precipitation changes over the three tropical regions in the Western Hemisphere.

The low-frequency variability of the Atlantic ITCZ is strongest and less predictable during boreal spring (Davey et al. 2002; Goddard and Mason 2002; Czaja 2004). The aim of this study is to understand the mechanisms responsible for the zonal variation of the Atlantic ITCZ and its relation to convection in equatorial South America in the spring season. Specifically, we use 15-yr (1979–93) satellite-measured OLR data (Liebmann and Smith 1996) to identify the dominant modes of convective variability over the equatorial Amazon and the tropical Atlantic. In addition, we use precipitation data from the Tropical Rainfall Measuring Mission (TRMM) satellite observations (Kummerow et al. 2000), which covers more recent years, to support our analysis based on the OLR data. Ocean surface winds from the Quick Scatterometer (QuikSCAT) satellite (Graf et al. 1998) are also employed to verify the surface signature of the convectively coupled Kelvin wave that links convection over South America and the tropical Atlantic. This study is among the first attempts to use satellite observations to detect the influence of convection over South America on the tropical Atlantic variability.

This paper is organized as follows. Section 2 provides a brief description of the datasets and analysis methods. The leading modes of variability of convection in equatorial South America and the tropical Atlantic are examined in section 3. Section 4 analyzes large-scale dynamical fields associated with the convectively coupled Kelvin wave, which originates from the Amazon convection and modulates the Atlantic ITCZ. Section 5 discusses the seasonal and interannual variability of the Kelvin wave. Our results are summarized and discussed in section 6.

2. Data and methods

For this study, we use the CDC's interpolated daily OLR data (Liebmann and Smith 1996) and the European Centre for Medium-Range Weather Forecasts (ECMWF) Re-Analysis (ERA) daily data to characterize convection and associated atmospheric dynamic fields in both equatorial South America and the tropical Atlantic. The OLR data are originally twice-daily measurements from the National Oceanic and Atmospheric Administration (NOAA) polar-orbiting satellites (Gruber and Krueger 1984) and interpolated into daily values (Liebmann and Smith 1996). The ERA daily data, including three-dimensional atmospheric wind fields and covering a 15-yr period (1979–93), are the averages of 4-times-daily data at 0000, 0600, 1200, and 1800 UTC. Both data are on a $2.5^\circ \times 2.5^\circ$ grid. We use the OLR data in the same period (1979–93) overlapping the ERA data.

Most previous studies of tropical waves and ITCZs use OLR as a proxy of deep convection (e.g., Wheeler and Kiladis 1999; Gu and Zhang 2001). Peak negative OLR anomalies, however, can lag peak deep convection by up to 12 h (Wheeler et al. 2000). In addition to the OLR and ERA data, we also use TRMM (Kummerow et al. 2000) and QuikSCAT (Graf et al. 1998) satellite data for more recent periods. The OLR mainly represents cirrus clouds and is also influenced by other large-scale atmospheric processes in addition to synoptic-scale disturbances (Gu and Zhang 2002). Precipitation data are more closely linked to convection and thus are an alternative indicator of the location and intensity of ITCZs (e.g., Zhang 2001). A 4-yr (2000–03) dataset of daily rain rate from the TRMM satellite is used to verify and compare to the results based on the OLR data. The TRMM rainfall data have been shown to effectively capture various equatorial waves (Cho et al. 2004). The data are the TRMM level-3 product (3B42) with a spatial coverage of 40°N – 40°S and a horizontal resolution of $1^\circ \times 1^\circ$ (Kummerow et al. 2000). Ocean surface winds measured by the SeaWinds scatterometer on the QuikSCAT satellite (Graf et al. 1998) are also

used to detect disturbances in the ocean surface associated with the equatorial wave. The data are 2 times daily at 0000 and 1200 UTC, respectively, on a $1^\circ \times 1^\circ$ grid. We use daily means for the same period as the TRMM data.

Two statistical methods are used to establish the relationship between convection in equatorial South America and that in the Atlantic ITCZ. One is the conventional empirical orthogonal function (EOF) analysis, and the other is linear regression. The former is able to objectively identify dominant variability of convection in the tropical South American–Atlantic sector. The latter is used to obtain OLR, precipitation, and atmospheric circulation anomalies that are associated with the tropical waves. Prior to the EOF analysis, the daily OLR and TRMM rain-rate data are processed through a Lanczos bandpass filter (2–25 days; Duchon 1979) to highlight synoptic-scale signals and exclude daily fluctuations and intraseasonal variations. Hovmöller diagrams are employed to identify convectively coupled tropical waves and to illustrate their propagation along the equator. Phase speed can be estimated from the longitude–time cross sections by analyzing the slope of lines of peak convection.

3. Kelvin wave linking the Atlantic ITCZ to Amazon convection

Whether the eastward-propagating convection shown in Fig. 2 is representative of coherent variations of convection in equatorial South America and the tropical Atlantic is examined by an EOF analysis on filtered (2–25 days) daily OLR anomalies over the two regions (10°S – 10°N , 0° – 80°W) for MAM 1979–93. The first two EOFs are distinct and well separated from the rest of the modes based on a rule of thumb suggested by North et al. (1982). The two modes explain 15.4% and 12.1% of the total variance, respectively, over the equatorial Amazon–tropical Atlantic sector. Their spatial patterns (Fig. 3) are shown in the form of correlation coefficients between filtered OLR anomalies and the time series of corresponding EOF modes. The first mode (Fig. 3a) is characterized by a center of negative correlations in the coast of northeast Brazil and two centers of positive correlations in western equatorial South America and the eastern tropical Atlantic, respectively. The tripole pattern suggests that stronger convection in the western Atlantic and northeast Brazil tends to be associated with weaker convection in the equatorial western Amazon and eastern Atlantic. The second mode (Fig. 3b) displays a zonal dipole in equatorial South America and the tropical Atlantic (Fig. 3b). This mode depicts an out-of-phase relationship between convection in the central Amazon and tropical Atlantic, indicating that a

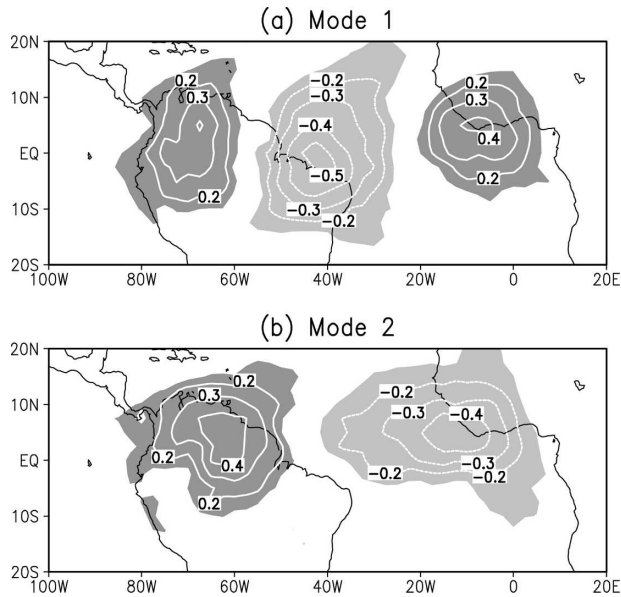


FIG. 3. Spatial patterns of the first two EOF modes of filtered daily OLR for MAM 1979–93. The maps are shown in the form of correlation coefficients between filtered OLR anomalies and the time series of corresponding EOF mode. Contour interval is 0.1. Contours between -0.2 and 0.2 are omitted. Dark (light) shadings indicate positive (negative) correlations exceeding the 1% significance level as estimated by the Monte Carlo tests.

stronger ITCZ is related to weaker convection in the central Amazon.

The normalized time series of the two EOF modes are shown in Fig. 4a, as an example, for the period of 1

March–31 May 1993. Both time series display fluctuations on synoptic time scales. A spectrum analysis (not shown) reveals that the two modes are dominated by 6- and 7.5-day oscillations, respectively. Although the two modes are orthogonal, lead and lag correlations between the two EOF time series are highly significant when the first mode leads the second mode 1–2 days or lags 1–3 days, as shown in Fig. 4b. The correlations for mode 1 leading mode 2 are greater than those for mode 1 lagging mode 2, indicating that peak convection associated with mode 1 leads that associated with mode 2. The alternating positive and negative correlations with lag days suggest that both modes oscillate with a similar period around 6–8 days.

The west–east tripole (Fig. 3a) and dipole (Fig. 3b) structures of the leading EOF modes with the temporal variations peaking at 6- and 7.5-day oscillations (Fig. 4a) in the anomalous OLR field dominate the Atlantic ITCZ and Amazon convection on synoptic time scales and likely represent the zonal variation of the ITCZ. To illustrate the linkage between the Atlantic ITCZ and Amazon convection, we show in Fig. 5 the time evolution of total OLR fields associated with the two EOF modes. The daily OLRs are reconstructed from the 15-yr boreal spring (MAM) daily OLR via lead and lag multiple linear regressions against the two EOF time series. The composites correspond to a 1.5 standard deviation departure in both EOF time series. The day when convection in the western tropical Atlantic is strongest is defined as day 0. Three days before the

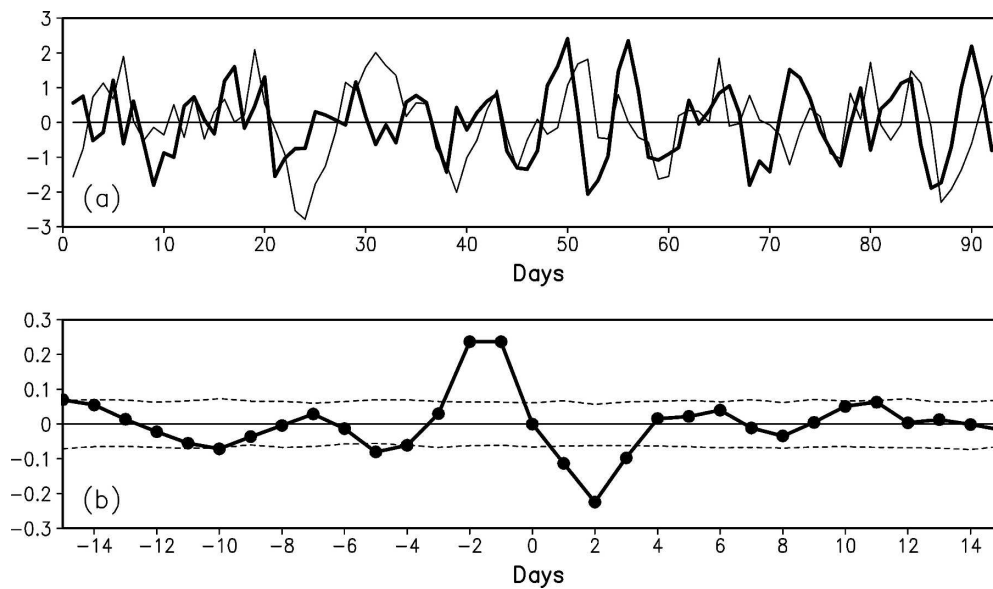


FIG. 4. (a) Normalized time series of the first (thick) and second (thin) EOF modes from 1 Mar to 31 May 1993. (b) Lead and lag correlations between the two EOF time series of the 15-yr MAM daily OLR from day -15 (mode 1 leading mode 2, 15 days) to day 15 (mode 1 lagging mode 2, 15 days). Dashed lines in (b) denote the 1% significance level as estimated by the Monte Carlo tests.

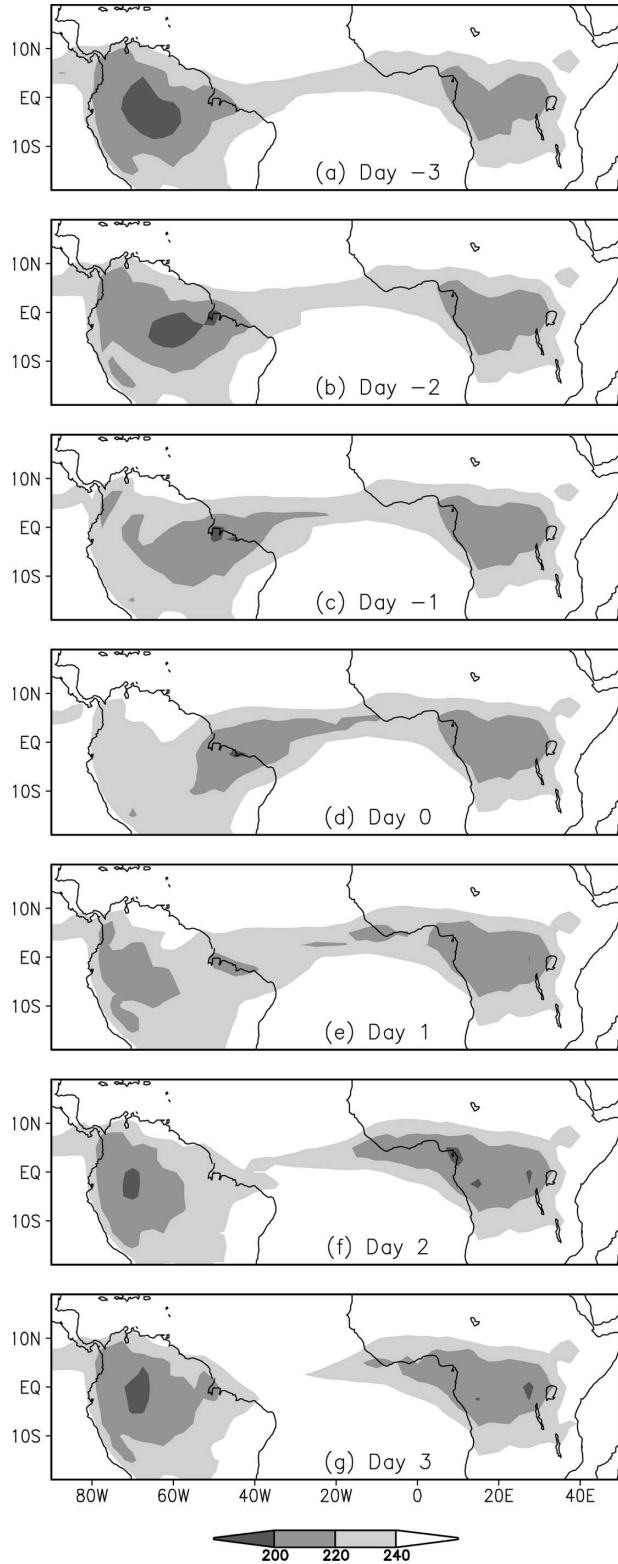


FIG. 5. Regression patterns of 15-yr MAM daily OLR against the two leading EOF time series with a 1.5 standard deviation departure. Composite maps are shown for OLR leading the strong convection in the western tropical Atlantic by (a) 3, (b) 2, (c) 1, and (d) 0 days and lagging by (e) 1, (f) 2, and (g) 3 days. Light, dark, and darker shadings indicate OLR below 240, 220, and 200 W m^{-2} , respectively.

strong ITCZ in the western Atlantic, the ITCZ is relatively weak (Fig. 5a). At day -3 , the strongest convection (minimum OLR) occurs in equatorial South America between 60° and 70°W . The center of the strongest convection over the land shifts toward the east and reaches the east coast at day -1 (Figs. 5b,c). The eastward-propagating lower OLR induces a strong ITCZ in the western Atlantic at day 0 (Fig. 5d). In the following 3 days the convective disturbance continues to move eastward and crosses the Atlantic (Figs. 5e–g). A strong ITCZ in the eastern Atlantic is thus established. In the meantime, a new center of strong convection forms in the western Amazon and then shifts eastward. The lead and lag composites of daily OLR clearly illustrate a life cycle of the zonal variation of convection in equatorial South America and the tropical Atlantic. The convective disturbance developed in equatorial South America at day -3 propagates eastward, leading to a strong western Atlantic ITCZ at days -1 and 0 and then a strong eastern Atlantic ITCZ at days 2 and 3. The observed time evolution of convection shown in Fig. 2 is similar to that reconstructed based on the two EOF modes (Fig. 5). The time series of the two EOF modes (Fig. 4a) are also consistent with the changes of the ITCZ location during 16–22 April 1993 (Fig. 2). The first mode displays a large peak on 19 April 1993 (day 50, Fig. 4a) corresponding to the strong ITCZ in the western Atlantic (Fig. 2). At day 52, the two modes show a large negative and positive peak, respectively, which account for the strong ITCZ in the eastern Atlantic on 21 April 1993. Therefore, the zonal variation of the Atlantic ITCZ is well captured by the two leading EOF modes. It is also obvious that during 16–22 April 1993 (days 47–53 in Fig. 4a) the first mode leads the second mode by 2 days, consistent with the lead and lag correlations (Fig. 4b).

Clearly, the eastward-propagating convection contributes directly to the zonal variation of the Atlantic ITCZ. The signals likely originate from deep convection in equatorial South America. Similar lead and lag regression OLR patterns associated with individual EOF modes also display the eastward-propagation feature (not shown). The average phase speed is around 15 m s^{-1} as estimated from Fig. 5. The tripole and dipole of OLR anomalies (Fig. 3) span equatorial South America and the Atlantic basin, which suggests that the two modes have zonal wavenumbers of 6 and 4, respectively. The eastward-propagating disturbances with such wave characteristics, detected by the method typically used for observing tropical waves (e.g., Dunkerton and Crum 1995; Cho et al. 2004), match those of the well-known Kelvin wave (Wheeler and Kiladis 1999). The convective disturbances with wavenumbers of 6

and 4 and periods of 6 and 7.5 days are identified as Kelvin wave signals above the 5% significance level in the wavenumber-frequency spectra of convectively coupled equatorial waves (Wheeler and Kiladis 1999, their Fig. 3). We thus suggest that deep convection in equatorial South America may generate convectively coupled Kelvin waves that propagate eastward, modulate convection in the tropical Atlantic, and result in a zonal variation of the Atlantic ITCZ.

4. Dynamical fields associated with the convectively coupled Kelvin wave

The Kelvin wave signal can be seen more clearly in an anomalous OLR field than in the total OLR field (Fig. 5). Figure 6 shows the OLR and surface wind anomalies obtained from the lead and lag linear regressions against the two EOF time series. At day -3 large negative OLR anomalies are found in equatorial South America centered at 60°W and positive OLR anomalies in the western Atlantic (Fig. 6a). Strong convection associated with the negative OLR anomalies crosses the equatorial Amazon at day -2 and the tropical Atlantic from day -1 to day 3. The anomalous peak convection (negative OLR) is stronger in the western Atlantic (Figs. 6c,d) than in the eastern Atlantic (Figs. 6f,g). Figure 6 also shows two centers of positive and negative OLR anomalies that develop in the western equatorial Amazon at day -1 and day 2, respectively, and then move eastward. The out-of-phase relation between convection in equatorial South America and the western Atlantic is observed throughout most of the 7-day period. The lead and lag composites of OLR anomalies illustrate clearly a life cycle of alternate strong and weak convective disturbances that are generated in equatorial South America and then propagate eastward across the tropical Atlantic and modulate the intensity and location of the ITCZ.

The changes in the surface wind are consistent with the eastward-propagating convective disturbances. Near the equator, the surface wind has a relatively large zonal component. Westerly wind anomalies are associ-

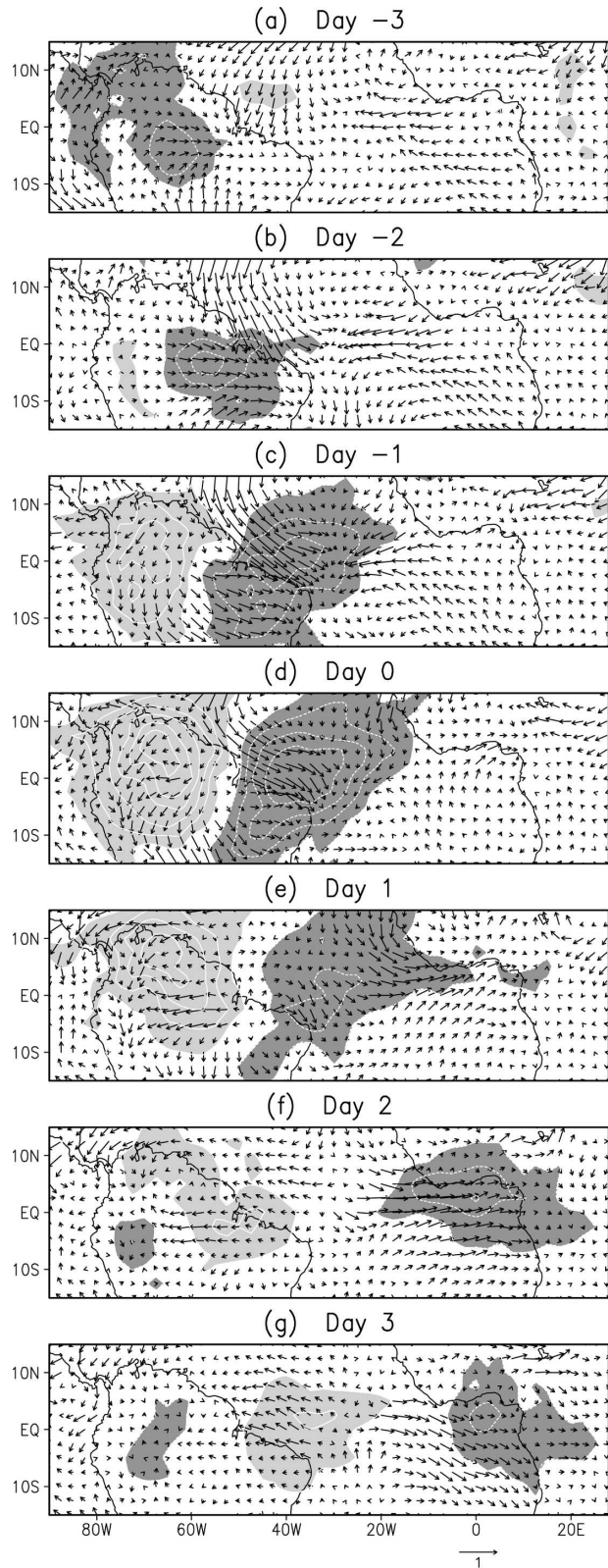


FIG. 6. Regression patterns of MAM OLR anomaly (contours) and surface wind anomaly at 10-m height (unit: m s^{-1} , vectors) associated with 1.5 standard deviation departure in the two EOF time series. Composite maps are shown for circulation leading strong convection in the western Atlantic by (a) 3, (b) 2, (c) 1, and (d) 0 days and lagging by (e) 1, (f) 2, and (g) 3 days. Dark and light shadings indicate negative and positive OLR anomalies exceeding 5 W m^{-2} , respectively. The contour interval is 5 W m^{-2} , starting from $\pm 10 \text{ W m}^{-2}$.

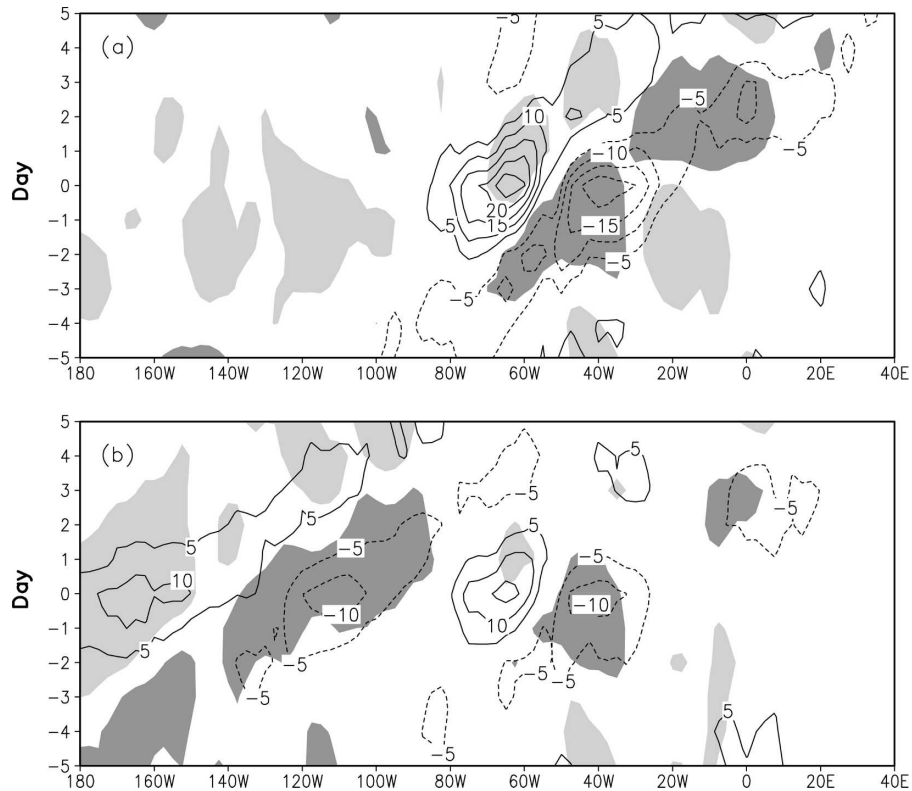


FIG. 7. Longitude–time diagram of daily OLR (contours) and surface zonal wind (shadings) anomalies at 10-m height along the equator associated with a 1.5 standard deviation departure in the time series of the two EOF modes based on the OLR data in (a) equatorial South America and the tropical Atlantic and (b) the entire equatorial Western Hemisphere. Contour interval is 5 W m^{-2} with negative values dashed. Zero contours are omitted. Dark and light shadings indicate the westerly and easterly zonal wind anomalies, respectively.

ated with negative OLR and easterlies are associated with positive OLR. This is one of the important features of the Kelvin wave (Wheeler and Kiladis 1999). In addition, the surface wind converges in the region of enhanced convection and diverges in the region of weakened convection, which is dynamically consistent with the OLR anomalies. The convectively coupled Kelvin wave is well detected in the lower-level wind field.

Figure 7a shows a Hovmöller diagram of the composite OLR and lower-level zonal wind anomalies along the equator from day -5 to day 5 , which are obtained in the same way as those in Fig. 6. Eastward-propagating signals in both OLR and zonal wind fields are clearly seen in South America and the Atlantic. Five days before the peak convection (large negative OLR anomaly) appears in the western Atlantic, negative OLR anomalies and associated convection first start over western equatorial South America (80°W , day -5). Two days later this anomaly signal propagates to the central Amazon (60°W , day -3). The OLR

anomalies are intensified with a maximum value exceeding 10 W s^{-1} . Five days later (day 0) the signal propagates to the western Atlantic between 20° and 50°W . The OLR anomalies are doubled over the ocean as compared to those in the central Amazon. At this time a strong ITCZ is located in the western Atlantic. As the anomalous convection continues to move eastward, positive OLR anomalies appear in the western Atlantic from day 2 to day 5 , which originally propagate from the central Amazon around 70°W at day -2 . During the 9-day period from day -4 to day 4 the negative OLR associated with the Kelvin wave travels from 80°W to 20°E across 100° in longitude with a phase speed equivalent to 14.3 m s^{-1} .

The zonal wind anomalies at 10-m height (shadings, Fig. 7a) are clearly associated with the eastward-propagating convection across the Atlantic basin. Easterly anomalies are found in the western Atlantic during days -5 and -4 preceding the anomalous convection center. When convection becomes stronger and the OLR anomalies are negative, the easterly wind

anomaly shifts to westerly. Therefore, surface westerly (easterly) anomalies are collocated with negative (positive) OLR anomalies. This configuration is consistent with the dynamic structure of the Kelvin wave (Straub and Kiladis 2002).

Whether the observed Kelvin wave originates from South America or from the Pacific is also examined in Fig. 7a. If the convectively coupled Kelvin wave originated from the Pacific, the coherent structure of zonal wind and OLR anomalies should also exist over the eastern Pacific. Although the OLR anomalies may first develop on the west coast of South America around 80°W, the zonal wind anomalies mainly start from the central Amazon, indicating that the Kelvin wave is excited in this region. Some easterly wind anomalies do exist in the central and eastern Pacific during day -4 and day 2. However, they are not along the line of maximum OLR and easterly anomalies in the South American-Atlantic sector. In addition, no significant OLR anomalies are found west of 80°W. The eastern tropical Pacific is a cold-tongue region where deep convection unlikely occurs except for strong El Niño years. Thus few convectively coupled Kelvin waves emerge to the west of 80°W.

A recent study of Mounier et al. (2007) on the West African monsoon shows that Kelvin wave detected over the Atlantic and Africa may propagate from the eastern Pacific in boreal summer when the Amazon is in its dry season and convection is relatively weak near the equator. Our EOF results (Fig. 3) indicate that there are no such significant OLR signals associated with Kelvin waves in the eastern Pacific in boreal spring. Whether this is due to an exclusion of the data from this region in the EOF analysis is examined by performing a similar EOF analysis of the OLR data except for the entire equatorial Western Hemisphere (10°S-10°N, 0°-180°). The spatial patterns of the second and fourth modes, which have high loadings in the tropical South American-Atlantic sector (not shown), are very similar to those of the two leading modes in Fig. 3 based only on the OLR data in equatorial South America and the tropical Atlantic. The temporal correlation between the first (second) EOF mode for the equatorial South American and the Atlantic domain and the second (fourth) EOF mode for the equatorial Western Hemisphere domain is 0.84 (0.65). The Hovmöller diagrams shown in Fig. 7 compare the composite OLR and surface zonal wind anomalies along the equator associated with the first and second EOFs for equatorial South America and the tropical Atlantic (Fig. 7a) to those with the second and fourth EOFs for the equatorial Western Hemisphere (Fig. 7b). For the latter (Fig. 7b), both OLR and zonal wind anomalies propagate east-

ward from west of the date line, indicating that in this case the Kelvin wave is indeed from the Pacific. However, the OLR anomalies over the Amazon and the tropical Atlantic in Fig. 7b are much weaker than those in Fig. 7a. This suggests that the Kelvin waves propagating from the Pacific have weaker signals than those excited by Amazon convection.

To further assess the Kelvin wave signatures in the upper level, Fig. 8 shows the composite of 200-hPa divergent wind anomalies and associated divergence field obtained by the lead and lag linear regressions against the two EOF time series based on the OLR in the equatorial South American and Atlantic domain. Upper-level outflow from the region of enhanced convection and inflow to the region of weakened convection are evident. The convergence (divergence) of the wind anomalies are consistent with the positive (negative) OLR anomalies and shift eastward with the Kelvin wave, suggesting a coupling between the Kelvin wave and deep convection. In the eastern Pacific positive OLR anomalies and divergent wind anomalies are found at day -3 and -2. These anomalies are stationary and show up only from day -4 (not shown) to -2, as compensation flows and a direct thermal response to convection over western equatorial South America. Figures 7a and 8 suggest that the convectively coupled Kelvin waves that predominately contribute to the zonal variation of the Atlantic ITCZ mainly originate from equatorial South America. Propagation of Kelvin waves from the Pacific, as shown in Fig. 7b, does not seem to dominate the zonal variation of the Atlantic ITCZ in boreal spring.

Convectively coupled Kelvin waves can also be detected with other satellite data, including the TRMM rain rate and the QuikSCAT ocean surface wind. They have relatively short records but are more reliable and objective in representing convection and surface wind. We perform the EOF analysis on the filtered TRMM daily rain rate in equatorial South America and the tropical Atlantic for spring 2000-03. The spatial patterns of the first two EOF modes (not shown) are very similar to those with the OLR data (Fig. 3). Figure 9 shows a Hovmöller diagram of precipitation and ocean surface zonal wind anomalies reconstructed based on the lead and lag linear regressions versus the two EOF time series of the TRMM rainfall. Eastward-propagating signals are easily identified in both precipitation and surface zonal wind fields to the east of 80°W. The rainfall anomalies start from the equatorial western Amazon, consistent with the OLR anomaly in Fig. 7a. Over the tropical Atlantic, the surface westerly (easterly) anomalies are to the west (east) of maximum precipitation. This feature is different from that between

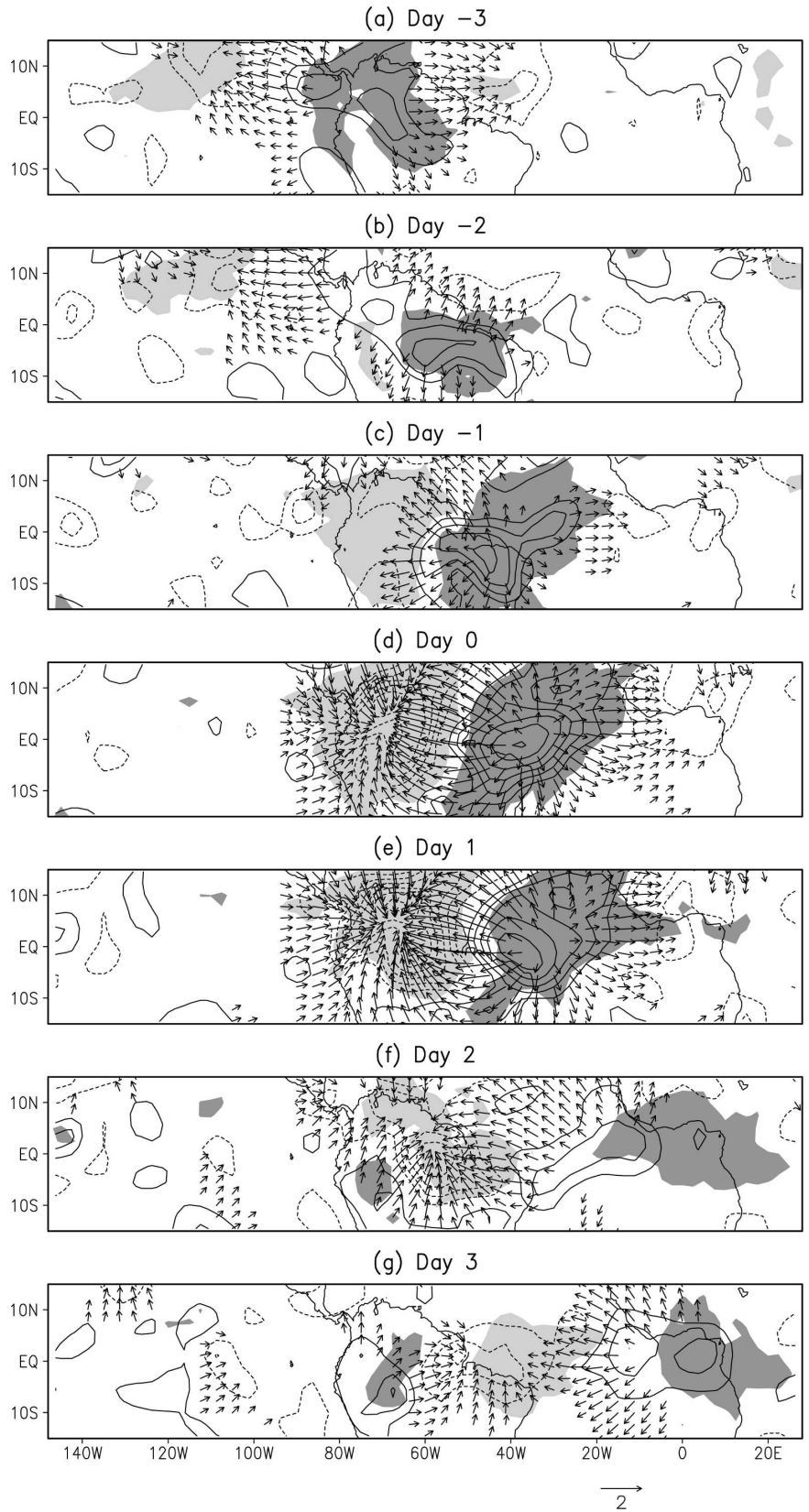


FIG. 8. Same as in Fig. 6 but for 200-hPa divergent wind (vectors) and divergence (contours). Contour interval is $0.5 \times 10^{-6} \text{ s}^{-1}$. Negative contours are dashed and zero contours are omitted. Shadings are the same as in Fig. 6.

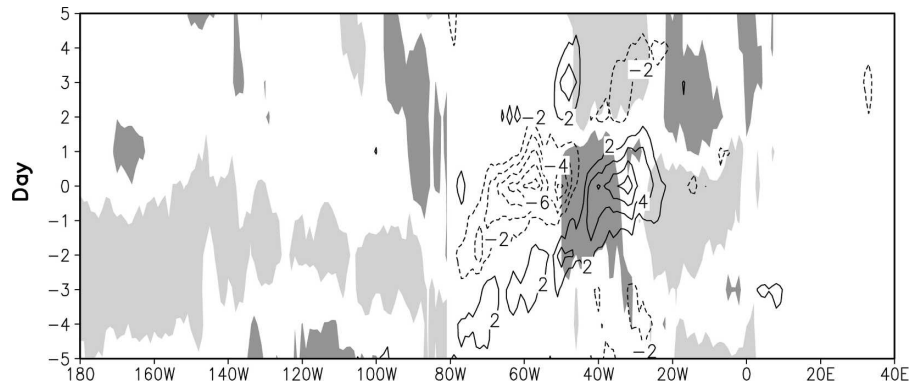


FIG. 9. Longitude–time diagram of TRMM daily rain rate (contours) and QuikSCAT ocean surface zonal wind (shadings) anomalies along the equator associated with a 1.5 standard deviation departure in the two EOF time series. Contour interval is 2 mm day^{-1} with negative values dashed. Zero contours are omitted. Dark and light shadings indicate the westerly and easterly zonal wind anomalies, respectively.

zonal wind and OLR anomalies (Fig. 7a). A comparison between Figs. 7a and 9 indicates that peak OLR is to the west of maximum rainfall and thus lags behind precipitation. In the Tropics high clouds lag deep convection (Tian et al. 2004) and propagate westward (Perez et al. 2006, manuscript submitted to *J. Atmos. Sci.*). This explains the observed difference between precipitation and OLR anomalies in relation to the surface zonal wind. Thus both the TRMM and QuikSCAT satellite observations also show a clear signal of convectively coupled Kelvin waves. The anomalous wind pattern expected from the Kelvin waves is absent in the eastern Pacific, which is consistent with the findings of Dunkerton and Crum (1995) and Wheeler et al. (2000). This again suggests that the Kelvin waves over the Atlantic predominantly originate from deep convection in South America instead of from the Pacific.

5. Seasonality and interannual variability

To examine the seasonal and interannual variability of the convectively coupled Kelvin wave, we apply the EOF analysis on the 15-yr filtered daily OLR instead of just MAM daily data. The EOF modes relevant to the Kelvin wave that we previously identified for spring also exist all year-round. In this case, they are the first and third modes as shown in Fig. 10. They explain, respectively, 18.5% and 9.9% of precipitation variance over the equatorial Amazon and the tropical Atlantic. The spatial patterns are similar to their corresponding modes in the spring season (Fig. 3). The first mode (Fig. 10a), however, concentrates more on the out-of-phase relationship between convection in the equatorial Amazon and western Atlantic. The loadings in the eastern Atlantic are relatively weak. The third mode fo-

cuses more on convection in the eastern Atlantic. Compared to the second mode of the spring season (Fig. 3b), the center of positive correlations is located in the western Atlantic rather than over the land. Figure 10 also indicates that the centers of positive and negative correlations shift slightly to the north, especially over the ocean. This may be largely due to the strong meridional migration of the ITCZ seasonally (Fig. 1).

Figure 11 shows the monthly mean daily variance of the two EOF time series for each year and also the 15-yr mean climatology. The 15-yr mean variance indicates a strong seasonality in both modes. The Kelvin

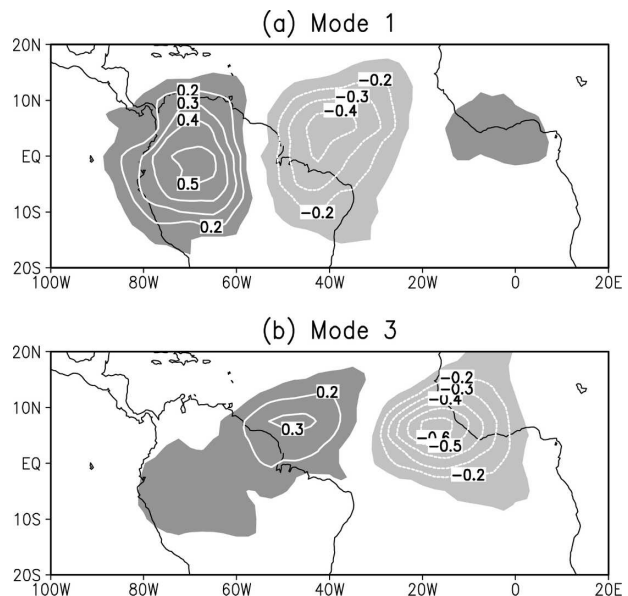


FIG. 10. Same as in Fig. 3 but for the first and third EOF modes of filtered daily OLR of 1979–93.

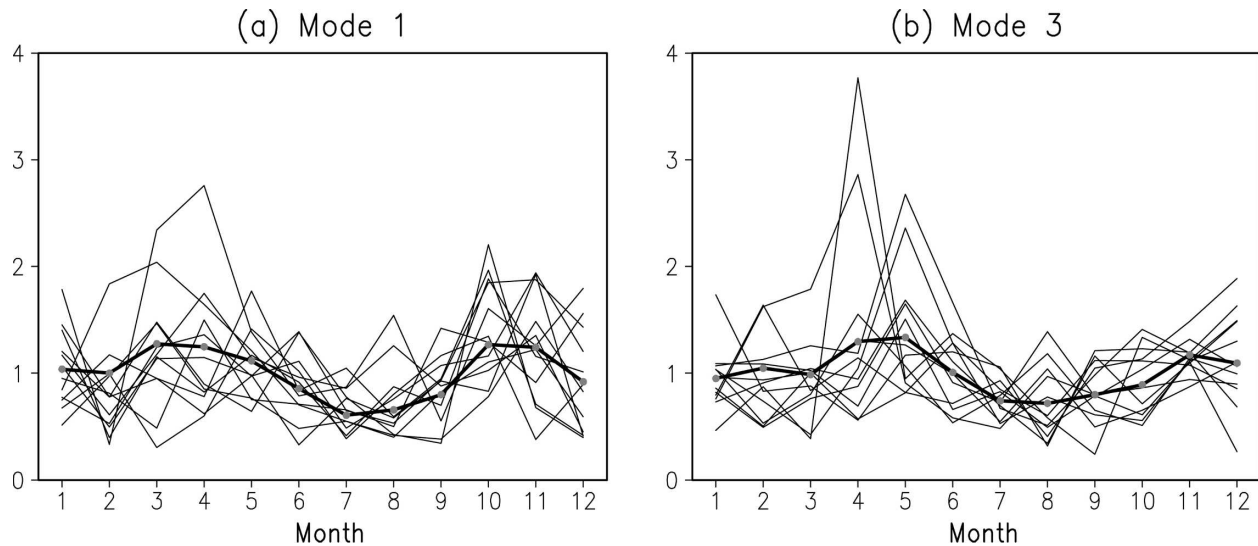


FIG. 11. Monthly mean daily variance of the normalized time series of (a) the first and (b) third EOF modes (thin lines) and 15-yr mean climatology (thick lines with dots).

wave has large amplitudes in boreal spring and fall and small amplitudes in summer. The variance in spring is comparable to that in fall for mode 1 (Fig. 11a) but stronger than that in fall for mode 3 (Fig. 11b). This is consistent with the finding of Roundy and Frank (2004) that the Kelvin wave has a maximum variability in spring and a secondary maximum in fall. The Kelvin wave also shows a strong interannual variability with largest year-to-year fluctuations in the spring season. We choose 6 yr with the highest variance and 6 yr with the lowest variance and composite spring seasonal mean precipitation and SST in the tropical Atlantic. During the years with the strongest Kelvin wave activities, coherent positive precipitation anomalies occur across the equatorial Amazon and over areas of warm SST anomalies in the tropical Atlantic and subtropical South Atlantic (not show). A study of the climate implication of the synoptic-scale Kelvin wave and how it links land convection to the tropical Atlantic variability is currently under way to disclose mechanisms responsible for the observed rainfall and SST changes.

6. Summary and conclusions

In this study, anomalies of daily OLR in March–May 1979–93 were examined over equatorial South America and the tropical Atlantic to elucidate the influence of Amazon convection on the Atlantic ITCZ on synoptic time scales. Observations show that convectively coupled Kelvin waves propagate eastward from equatorial South America to the tropical Atlantic and Africa in boreal spring. The Kelvin waves may originate from

deep convection in the equatorial Amazon and modulate convection and precipitation within the Atlantic ITCZ. Consequently, convection over equatorial South America induces a zonal variation of the ITCZ in the tropical Atlantic.

The convectively coupled Kelvin waves are characterized by a life cycle of 6–7.5 days, phase speeds of around 15 m s^{-1} , and zonal wavenumbers of 6 and 4. The Kelvin waves have coherent signatures in both the lower and upper atmosphere. The ERA data are employed to characterize the dynamical structure of the Kelvin wave. The surface zonal wind shifts from easterly to westerly at the time when convection becomes stronger. In the upper level, the zonal outflow from the region of enhanced convection is observed. A similar Kelvin wave signal is also identified in precipitation and ocean surface wind fields using the TRMM and QuikSCAT satellite observations. The Kelvin wave signal has a strong seasonality and interannual variability as well, especially in boreal spring.

This study has presented evidence that synoptic-scale variations of the Atlantic ITCZ and tropical African rainfall are directly linked to precipitation changes in South America during boreal spring. The convectively coupled Kelvin wave acts as a bridge linking convection and precipitation in these three tropical regions. The observed surface wind anomalies associated with the Kelvin wave also presumably influence surface fluxes and wind stress over the tropical Atlantic. How the Kelvin wave affects the ocean–atmosphere interaction in the tropical Atlantic, particularly on the interannual time scales, will be explored in our future work as a step

toward a clearer understanding of strong boreal spring climate variability of the tropical Atlantic ITCZ and SST.

Acknowledgments. This study was supported by the NASA QuikSCAT, NOAA Pan American Climate Studies (PACS), and NSF Climate and Large-Scale Dynamics programs. We thank Drs. George N. Kiladis, Robert E. Dickinson, and an anonymous reviewer for their insightful and constructive comments and suggestions. We thank Drs. W. Timothy Liu and Wenqing Tang for access to the reprocessed QuikSCAT data, Ms. Mingxuan Chen for assisting with the TRMM data, and Mrs. Susan Ryan for editorial assistance. The interpolated OLR data were provided by the NOAA/OAR/ESRL PSD, Boulder, Colorado, and are available from their Web site at <http://www.cdc.noaa.gov>.

REFERENCES

- Biasutti, M., D. S. Battisti, and E. S. Sarachik, 2003: The annual cycle over the tropical Atlantic, South America, and Africa. *J. Climate*, **16**, 2491–2508.
- , —, and —, 2005: Terrestrial influence on the annual cycle of the Atlantic ITCZ in an AGCM coupled to a slab ocean model. *J. Climate*, **18**, 211–228.
- Chang, P., L. Ji, and H. Li, 1997: A decadal climate variation in the tropical Atlantic Ocean from thermodynamic air–sea interactions. *Nature*, **385**, 516–518.
- , R. Saravanan, L. Ji, and G. C. Hegerl, 2000: The effect of local sea surface temperatures on atmospheric circulation over the tropical Atlantic sector. *J. Climate*, **13**, 2195–2216.
- Chiang, J. C. H., Y. Kushnir, and S. E. Zebiak, 2000: Interdecadal changes in eastern Pacific ITCZ variability and its influence on the Atlantic ITCZ. *Geophys. Res. Lett.*, **27**, 3687–3690.
- , —, and A. Giannini, 2002: Deconstructing Atlantic inter-tropical convergence zone variability: Influence of the local cross-equatorial sea surface temperature gradient and remote forcing from the eastern equatorial Pacific. *J. Geophys. Res.*, **107**, 4004, doi:10.1029/2000JD000307.
- Cho, H.-K., K. P. Bowman, and G. R. North, 2004: Equatorial waves including the Madden–Julian oscillation in TRMM rainfall and OLR data. *J. Climate*, **17**, 4387–4406.
- Cobb, K. M., C. D. Charles, and D. E. Hunter, 2001: A central tropical Pacific coral demonstrates Pacific, Indian, and Atlantic decadal climate connections. *Geophys. Res. Lett.*, **28**, 2209–2212.
- Czaja, A., 2004: Why is north tropical Atlantic SST variability stronger in boreal spring? *J. Climate*, **17**, 3017–3025.
- , P. van der Vaart, and J. Marshall, 2002: A diagnostic study of the role of remote forcing in tropical Atlantic variability. *J. Climate*, **15**, 3280–3290.
- Davey, M. K., and Coauthors, 2002: STOIC: A study of coupled model climatology and variability in tropical ocean regions. *Climate Dyn.*, **18**, 403–420.
- Dima, M., N. Rimbu, S. Stefan, and I. Dima, 2001: Quasi-decadal variability in the Atlantic basin involving tropics–midlatitudes and ocean–atmosphere interactions. *J. Climate*, **14**, 823–832.
- Duchon, C. E., 1979: Lanczos filtering in one and two dimensions. *J. Appl. Meteor.*, **18**, 1016–1022.
- Dunkerton, T. J., and F. X. Crum, 1995: Eastward propagating ~2- to 15-day equatorial convection and its relation to the tropical intraseasonal oscillation. *J. Geophys. Res.*, **100**, 25 781–25 790.
- Enfield, D. B., 1996: Relationships of inter-American rainfall to tropical Atlantic and Pacific SST variability. *Geophys. Res. Lett.*, **23**, 3305–3308.
- Fu, R., R. E. Dickinson, M. Chen, and H. Wang, 2001: How do tropical sea surface temperatures influence the seasonal distribution of precipitation in the equatorial Amazon? *J. Climate*, **14**, 4003–4026.
- Goddard, L., and S. J. Mason, 2002: Sensitivity of seasonal climate forecasts to persisted SST anomalies. *Climate Dyn.*, **19**, 619–631.
- Graf, J., C. Sasaki, C. Winn, W. T. Liu, W. Tsai, M. Freilich, and D. Long, 1998: NASA Scatterometer Experiment. *Acta Astronaut.*, **43**, 397–407.
- Gruber, A., and A. F. Krueger, 1984: The status of the NOAA outgoing longwave radiation data set. *Bull. Amer. Meteor. Soc.*, **65**, 958–962.
- Gu, G., and C. Zhang, 2001: A spectrum analysis of synoptic-scale disturbances in the ITCZ. *J. Climate*, **14**, 2725–2739.
- , and —, 2002: Westward-propagating synoptic-scale disturbances and the ITCZ. *J. Atmos. Sci.*, **59**, 1062–1075.
- Hagos, S. M., and K. H. Cook, 2005: Influence of surface processes over Africa on the Atlantic marine ITCZ and South American precipitation. *J. Climate*, **18**, 4993–5010.
- Hastenrath, S., and L. Heller, 1977: Dynamics of climate hazards in northeast Brazil. *Quart. J. Roy. Meteor. Soc.*, **103**, 77–92.
- Huang, B., P. S. Schopf, and Z. Pan, 2002: The ENSO effect on the tropical Atlantic variability: A regionally coupled model study. *Geophys. Res. Lett.*, **29**, 2039, doi:10.1029/2002GL014872.
- Janicot, S., A. Harzallah, B. Fontaine, and V. Moron, 1998: West African monsoon dynamics and eastern equatorial Atlantic and Pacific SST anomalies (1970–88). *J. Climate*, **11**, 1874–1882.
- Kummerow, C., and Coauthors, 2000: The status of the Tropical Rainfall Measuring Mission (TRMM) after two years in orbit. *J. Appl. Meteor.*, **39**, 1965–1982.
- Lamb, P. J., 1978: Large-scale tropical Atlantic surface circulation patterns associated with Saharan weather anomalies. *Tellus*, **30**, 240–251.
- Li, T., and S. G. H. Philander, 1997: On the seasonal cycle of the equatorial Atlantic Ocean. *J. Climate*, **10**, 813–817.
- Liebmann, B., and C. A. Smith, 1996: Description of a complete (interpolated) outgoing longwave radiation dataset. *Bull. Amer. Meteor. Soc.*, **77**, 1275–1277.
- Liu, Z., Q. Zhang, and L. Wu, 2004: Remote impact on tropical Atlantic climate variability: Statistical assessment and dynamic assessment. *J. Climate*, **17**, 1529–1549.
- Mitchell, T. P., and J. M. Wallace, 1992: The annual cycle in equatorial convection and sea surface temperature. *J. Climate*, **5**, 1140–1156.
- Mounier, F., G. N. Kiladis, and S. Janicot, 2007: Analysis of the dominant mode of convectively coupled Kelvin waves in the West African monsoon. *J. Climate*, in press.
- Moura, A. D., and J. Shukla, 1981: On the dynamics of droughts in northeast Brazil: Observations, theory, and numerical experiments with a general circulation model. *J. Atmos. Sci.*, **38**, 2653–2675.

- North, G. R., T. L. Bell, R. F. Cahalan, and F. J. Moeng, 1982: Sampling errors in the estimation of empirical orthogonal functions. *Mon. Wea. Rev.*, **110**, 699–706.
- Okumura, Y., and X.-P. Xie, 2004: Interaction of the Atlantic equatorial cold tongue and the African monsoon. *J. Climate*, **17**, 3589–3602.
- , —, A. Numaguti, and Y. Tanimoto, 2001: Tropical Atlantic air–sea interaction and its influence on the NAO. *Geophys. Res. Lett.*, **28**, 1507–1510.
- Poveda, G., and O. J. Mesa, 1997: Feedbacks between hydrological processes in tropical South America and large-scale ocean–atmospheric phenomena. *J. Climate*, **10**, 2690–2702.
- Rajagopalan, B., Y. Kushnir, and Y. M. Tourre, 1998: Observed decadal midlatitude and tropical Atlantic climate variability. *Geophys. Res. Lett.*, **25**, 3967–3970.
- Robertson, A. W., C. R. Mechoso, and Y. J. Kim, 2000: The influence of Atlantic sea surface temperature anomalies on the North Atlantic Oscillation. *J. Climate*, **13**, 122–138.
- , S. Kirshner, and P. Smyth, 2004: Downscaling of daily rainfall occurrence over northeast Brazil using a Hidden Markov Model. *J. Climate*, **17**, 4407–4424.
- Roundy, P. E., and W. M. Frank, 2004: A climatology of waves in the equatorial region. *J. Atmos. Sci.*, **61**, 2105–2132.
- Ruiz-Barradas, A., J. A. Carton, and S. Nigam, 2003: Role of the atmosphere in climate variability of the tropical Atlantic. *J. Climate*, **16**, 2052–2065.
- Saravanan, R., and P. Chang, 2000: Interaction between tropical Atlantic variability and El Niño–Southern Oscillation. *J. Climate*, **13**, 2177–2194.
- Serra, Y. L., and R. A. Houze Jr., 2002: Observations of variability on synoptic timescales in the east Pacific ITCZ. *J. Atmos. Sci.*, **59**, 1723–1743.
- Straub, K. H., and G. N. Kiladis, 2002: Observations of a convectively coupled Kelvin wave in the eastern Pacific ITCZ. *J. Atmos. Sci.*, **59**, 30–53.
- Tian, B., B. J. Soden, and X. Wu, 2004: Diurnal cycle of convection, clouds, and water vapor in the tropical upper troposphere: Satellites versus a general circulation model. *J. Geophys. Res.*, **109**, D10101, doi:10.1029/2003JD004117.
- Uvo, C. B., C. A. Repelli, S. E. Zebiak, and Y. Kushnir, 1998: The relationships between tropical Pacific and Atlantic SST and Northeast Brazil monthly precipitation. *J. Climate*, **11**, 551–562.
- Wheeler, M., and G. N. Kiladis, 1999: Convectively coupled equatorial waves: Analysis of clouds and temperature in the wave-number–frequency domain. *J. Atmos. Sci.*, **56**, 374–399.
- , —, and P. J. Webster, 2000: Large-scale dynamical fields associated with convectively coupled equatorial waves. *J. Atmos. Sci.*, **57**, 613–640.
- Xie, S.-P., 1999: A dynamic ocean–atmosphere model of the tropical Atlantic decadal variability. *J. Climate*, **12**, 64–70.
- , and Y. Tanimoto, 1998: A pan-Atlantic decadal climate oscillation. *Geophys. Res. Lett.*, **25**, 2185–2188.
- , and J. A. Carton, 2004: Tropical Atlantic variability: Patterns, mechanisms, and impacts. *Earth Climate: The Ocean–Atmosphere Interaction*, *Geophys. Monogr.*, Vol. 147, Amer. Geophys. Union, 121–142.
- Zhang, C., 2001: Double ITCZs. *J. Geophys. Res.*, **106**, 11 785–11 792.